



Erratum: Kinematics of dwarf galaxies in gas-rich groups, and the survival and detectability of tidal dwarf galaxies

by Sarah M. Sweet,¹★ Michael J. Drinkwater,² Gerhard Meurer,^{3,4} Virginia Kilborn,⁵ Fiona Audcent-Ross,^{3,4} Holger Baumgardt² and Kenji Bekki^{3,4}

¹Research School of Astronomy and Astrophysics, The Australian National University, Cotter Road, Weston Creek, ACT 2611, Australia

²School of Mathematics and Physics, University of Queensland, QLD 4072, Australia

³School of Physics, University of Western Australia, 35 Stirling Highway, Crawley, WA 6009, Australia

⁴International Centre for Radio Astronomy Research, ICRAR M468, 35 Stirling Highway, Crawley, WA 6009, Australia

⁵Centre for Astrophysics & Supercomputing, Swinburne University of Technology, Mail number H30, PO Box 218, Hawthorn, Victoria 3122, Australia

Key words: errata, addenda – galaxies: abundances – galaxies: dwarf – galaxies: groups: general – galaxies: interactions – galaxies: kinematics and dynamics – dark matter.

The paper ‘Kinematics of dwarf galaxies in gas-rich groups, and the survival and detectability of tidal dwarf galaxies’ was published in Monthly Notices of Royal Astronomical Society (Sweet et al. 2016). The line fluxes presented in that paper were incorrect due to an error in the flux calibration. In this erratum, we correct the line fluxes and the analysis that follows.

In Section 2 (final paragraph), the polynomial fit to $\log(q)$ as a function of R -band absolute magnitude M_R now takes the form $\log(q) = 7.574 + 0.111 M_R + 4.599 \times 10^{-3} \times M_R^2$.

In Fig. 1, we show the corrected luminosity–metallicity relation. Both tidal dwarf galaxy (TDG) candidates J1051–17:g11 and J1403–06:g1 identified in the paper now fall below the diagnostic line, so there are no strong TDG candidates in our DEIMOS sample based on our definition from Sweet et al. (2014) ($12 + \log(\text{O}/\text{H}) > 8.6$ and more than 3σ above SDSS).

In Table 1, we have updated columns (12)–(18) with correct line fluxes, ionization parameter and metallicity. Fig. 3 has also been updated; the results in that figure are unchanged.

We thank Emma Ryan-Weber for pointing out the error.

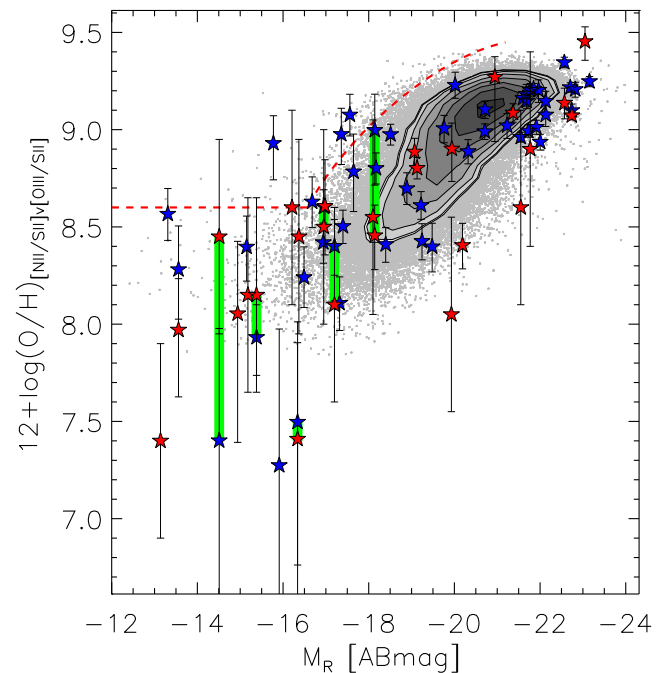


Figure 1. Luminosity–metallicity relation for the full sample of galaxies. Blue stars are existing WiFeS measurements from Sweet et al. (2014). Red stars are DEIMOS measurements. Green bars connect WiFeS and DEIMOS metallicities for the six galaxies that have measurements from both instruments. Grey points and contours depict SDSS star-forming galaxies, while the red dashed line indicates our strong TDG candidate diagnostic. Galaxies above this line are more than 3σ above the typical metallicity for their luminosity and hence candidate TDGs. None of the galaxies with DEIMOS metallicities meet this criterion.

* E-mail: sarah@sarahsweet.com.au

Table 1. Measured quantities for group member galaxies, including new group members. Columns (1) to (11). Columns: (1) SINGG name; (2) right ascension; (3) declination; (4) effective radius; (5) ratio of major to minor axes; (6) position angle; (7) velocity correction $\sin(i)\cos(\phi)$; (8) *R*-band extinction-corrected magnitude; (9) scalelength; (10) central surface luminosity; (11) heliocentric velocity.

(1) HIPASS+	(2) RA (h m s)	(3) Dec. (d m s)	(4) Reff (arcsec)	(5) a/b	(6) PA (°)	(7) Corr.	(8) M _R (mag)	(9) r ₀ (kpc)	(10) I ₀ (L _⊙ kpc ⁻¹)	(11) V _{hel} (km s ⁻¹)
J0443–05:S3	04 44 11.67	–05 14 38.31	04.79 ± 0.19	1.86	19	0.883	–19.93 ± 0.19	1.809	2.3E+8	4591
J0443–05:S4	04 44 05.54	–05 25 46.50	04.95 ± 0.12	1.6	120	0.537	–19.07 ± 0.12	1.048	5.9E+8	4774
J1051–17:S3	10 51 35.94	–16 59 16.80	06.61 ± 0.05	1.02	74	0.048	–18.14 ± 0.05	2.232	4.7E+7	5969
J1051–17:S4	10 51 26.01	–17 05 03.61	03.48 ± 0.09	1.4	164	0.661	–16.34 ± 0.09	0.837	7.5E+7	5465
J1051–17:S5	10 51 50.91	–16 58 31.64	03.58 ± 0.06	1.75	29	0.865	–17.20 ± 0.06	0.842	1.9E+8	5465
J1051–17:S6	10 51 42.78	–17 06 34.59	02.11 ± 0.04	1.29	40	0.422	–16.95 ± 0.04	0.492	3.0E+8	5648
J1051–17:S7	10 51 33.36	–17 08 36.63	04.18 ± 0.12	1.53	49	0.802	–16.94 ± 0.12	0.799	1.2E+8	5374
J1051–17:S8	10 51 25.92	–17 08 16.44	04.47 ± 0.10	3.07	63	0.927	–18.17 ± 0.04	0.804	7.5E+8	5294
J1051–17:g04	10 51 39.679	–17 03 34.16	02.97 ± 0.14	1.06	43	0.21	–18.10 ± 0.05	1.45	5.0E+7	5535
J1051–17:g07	10 51 43.698	–17 01 42.99	03.34 ± 0.09	1.12	42	0.3	–16.21 ± 0.08	0.95	4.0E+7	6166
J1051–17:g11	10 51 40.051	–16 57 30.94	01.95 ± 0.13	1	47	0.027	–16.37 ± 0.11	0.28	1.3E+9	5371
J1051–17:g13	10 51 41.602	–17 05 20.16	01.52 ± 0.16	1.05	42	0.21	–14.94 ± 0.21	0.685	8.0E+6	5577
J1051–17:g15	10 51 33.286	–17 08 19.17	05.26 ± 0.85	1.05	42	0.21	–15.18 ± 0.81	2.63	4.0E+6	5225
J1059–09:S2	10 59 06.77	–09 45 04.38	11.72 ± 0.24	1.36	131	0.056	–20.19 ± 0.24	5.271	4.7E+7	8013
J1059–09:S5	10 59 30.98	–09 44 25.26	09.11 ± 0.13	2.84	75	0.968	–19.94 ± 0.13	2.973	2.4E+8	7926
J1059–09:S7	10 59 21.31	–09 47 50.49	02.50 ± 0.15	1.59	115	0.167	–19.13 ± 0.15	0.761	1.2E+9	7862
J1059–09:S8	10 59 01.73	–09 52 46.76	03.47 ± 0.40	1.81	155	0.702	–16.98 ± 0.40	1.028	9.4E+7	8260
J1059–09:S9	10 58 44.69	–09 53 28.60	01.99 ± 0.08	1.39	45	0.604	–16.63 ± 0.08	0.63	2.0E+8	8475
J1059–09:S10	10 59 02.64	–09 53 19.90	03.47 ± 0.01	1.2	40	0.746	–20.95 ± 0.01	4.11	5.0E+7	8219
J1403–06:S3	14 03 13.48	–06 06 24.17	04.18 ± 0.85	1.03	14	0.158	–15.38 ± 0.85	0.448	7.5E+7	2753
J1403–06:S4	14 03 34.62	–06 07 59.27	05.96 ± 0.86	1.43	123	0.731	–14.51 ± 0.86	0.961	1.4E+7	2671
J1403–06:g1	14 03 22.475	–06 00 44.24	03.57 ± 0.36	2.04	46	0.76	–13.58 ± 1.39	2.51	6.3E+6	2692

Table 1. Measured quantities for group member galaxies, including new group members. Columns (12)–(22). (12–16) observed flux for various emission lines in units of 10^{-18} erg s⁻¹ cm⁻²: [O III] λ 5006.9, [N II] λ 6583.4, [S II] λ 6717.0+6731.3; (17) estimated ionization parameter based on Dopita et al. (2013) interpolation if [O III] available, or on M_R–log(*q*) relation of other galaxies in this sample otherwise; (18) 12+log(O/H) using Dopita et al. (2013) calibration; (19) membership of sample A (based on quality of rotation curve) is indicated here by the letter ‘A’; (20) *R*-band mass-to-light ratio; (21) modelled rotational velocity at *r*_{turn}; (22) tidal radius.

(1) HIPASS+	(12) H β	(13) [O III]	(14) H α	(15) [N II]	(16) [S II]	(17) log(<i>q</i>)	(18) 12+log(O/H)	(19) A	(20) M/L (M _⊙ /L _⊙)	(21) V _{rot} (km/s)	(22) r _{tidal} (arcsec)
J0443–05:S3			6.8 ± 1.4	0.5 ± 0.3	2.3 ± 1.0	7.19	8.05± ^{0.5} _{0.5}	A	4.15	120	89
J0443–05:S4		13.5 ± 4.4	118.0 ± 0.6	31.8 ± 0.3	47.9 ± 1.0	6.84	8.89± ^{0.08} _{0.07}	A	0.55	31.6	16
J1051–17:S3		3.7 ± 0.3	12.6 ± 0.2	1.9 ± 0.1	5.8 ± 0.7	6.73	8.46± ^{0.18} _{0.15}			3.8	37
J1051–17:S4		2.6 ± 0.3	6.6 ± 0.1	0.2 ± 0.1	2.7 ± 0.8	6.64	7.41± ^{2.93} _{0.6}	A	0.58	12.2	16
J1051–17:S5			20.6 ± 0.3	1.9 ± 0.2	8.0 ± 0.4	7.02	8.1± ^{0.5} _{0.5}	A	0.51	24.9	47
J1051–17:S6			102.8 ± 1.2	14.3 ± 0.4	32.1 ± 1.3	7.01	8.5± ^{0.5} _{0.5}	A	0.25	8.1	8
J1051–17:S7								A	0.03	3.8	8
J1051–17:S8			3.2 ± 0.1	2.6 ± 0.1				A	0.14	27.4	23
J1051–17:g04			12.5 ± 0.2	4.3 ± 0.2	9.9 ± 0.4	6.9	8.55± ^{0.5} _{0.5}			14.3	29
J1051–17:g07			9.7 ± 0.3	1.6 ± 0.3	3.2 ± 1.6	6.9	8.6± ^{0.5} _{0.5}			13.8	25
J1051–17:g11			0.5 ± 0.1	0.4 ± 0.1	1.0 ± 0.1	6.9	8.45± ^{0.5} _{0.5}			20.1	27
J1051–17:g13		6.5 ± 1.1	7.6 ± 0.2	0.4 ± 0.1	2.2 ± 0.4	6.91	8.05± ^{0.66} _{0.38}			12	7
J1051–17:g15			8.3 ± 0.1	1.2 ± 0.1	5.2 ± 1.0	6.82	8.45± ^{0.5} _{0.5}			0	4
J1059–09:S2		20.7 ± 3.3	27.8 ± 0.4	4.1 ± 0.2	11.5 ± 0.8	6.92	8.41± ^{0.13} _{0.11}			33.1	31
J1059–09:S5	1.9 ± 0.1	7.1 ± 0.5	11.4 ± 0.3	1.2 ± 0.1	1.0 ± 0.1			A	0.28	41.4	40
J1059–09:S7	5.3 ± 0.1	7.2 ± 1.1	45.6 ± 0.7	10.3 ± 0.2	16.8 ± 0.6	6.86	8.8± ^{0.05} _{0.06}			7.4	8
J1059–09:S8	0.7 ± 0.1	1.6 ± 0.8	4.5 ± 0.2	0.8 ± 0.1	1.8 ± 0.3	6.88	8.61± ^{0.25} _{0.24}	A	0.4	14.1	29
J1059–09:S9	0.7 ± 0.1	3.6 ± 0.7	6.0 ± 0.2	0.4 ± 0.1	2.7 ± 0.3	6.75	7.97± ^{0.34} _{0.26}	A	0.43	14.1	45
J1059–09:S10		2.5 ± 0.4		7.1 ± 0.7	2.1 ± 1.0	8.49	9.27± ^{0.33} _{0.11}			0.4	102
J1403–06:S3			6.5 ± 0.1	0.4 ± 0.1	1.7 ± 0.1	6.95	8.15± ^{0.5} _{0.5}			4.7	11
J1403–06:S4			1.8 ± 0.1	0.2 ± 0.0	0.4 ± 0.1	6.93	8.45± ^{0.5} _{0.5}			4.8	10
J1403–06:g1	1.6 ± 0.1		15.6 ± 0.1	4.1 ± 0.1	5.1 ± 0.1	6.91	7.4± ^{0.5} _{0.5}			32.5	2

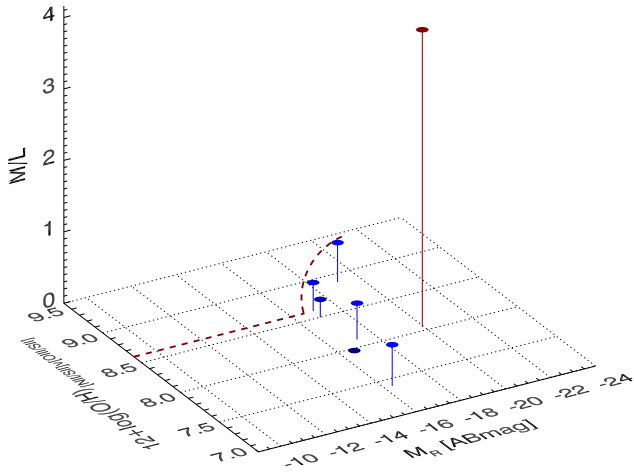


Figure 3. Mass-to-light ratio as a function of the luminosity–metallicity relation for the galaxies in our sample that have reliable mass-to-light ratios. The data points are colour-coded by mass-to-light ratio, with red being the highest and blue the lowest in this sample. The red dashed line is the strong TDG candidate diagnostic line as defined in Sweet et al. (2014).

REFERENCES

- Dopita M. A., Sutherland R. S., Nicholls D. C., Kewley L. J., Vogt F. P. A., 2013, *ApJS*, 208, 10
 Sweet S. M., Drinkwater M. J., Meurer G., Bekki K., Dopita M. A., Kilborn V., Nicholls D. C., 2014, *ApJ*, 782, 35
 Sweet S. M., Drinkwater M. J., Meurer G., Kilborn V., Audcent-Ross F., Baumgardt H., Bekki K., 2016, *MNRAS*, 455, 2508

This paper has been typeset from a \LaTeX file prepared by the author.